

Effect of post-treatments on the photocatalytic activity of $\text{Sm}_2\text{Ti}_2\text{S}_2\text{O}_5$ for the hydrogen evolution reaction

Cite this: *Phys. Chem. Chem. Phys.*, 2014, 16, 12051

Wen Zhao,^a Kazuhiko Maeda,^{†ab} Fuxiang Zhang,^{‡a} Takashi Hisatomi^a and Kazunari Domen^{*a}

The oxysulphide photocatalyst $\text{Sm}_2\text{Ti}_2\text{S}_2\text{O}_5$ was synthesized by sulphurizing an amorphous $\text{Sm}_2\text{Ti}_2\text{O}_7$ prepared using a polymerized complex method under a H_2S flow and was used as a H_2 evolution photocatalyst in the sacrificial H_2 evolution and Z-scheme water splitting reactions. The H_2 evolution activity of Rh-loaded $\text{Sm}_2\text{Ti}_2\text{S}_2\text{O}_5$ was improved by annealing with sulphur powder and etching with nitric acid. Characterization using XRD, SEM, DRS and XPS suggested that annealing with sulphur decreased the density of the reduced Ti species in $\text{Sm}_2\text{Ti}_2\text{S}_2\text{O}_5$ and etching with nitric acid removed the amorphous phases and excessive sulphur species on the surface. After the two post-treatments, platinized $\text{Sm}_2\text{Ti}_2\text{S}_2\text{O}_5$ combined with rutile-type TiO_2 and NaI showed activity for Z-scheme water splitting under UV irradiation. Although UV irradiation was necessary owing to the use of TiO_2 , this work provided the first evidence that an oxysulphide photocatalyst was applicable to Z-scheme water splitting.

Received 5th November 2013,
Accepted 2nd December 2013

DOI: 10.1039/c3cp54668c

www.rsc.org/pccp

Introduction

Photocatalytic water splitting has attracted worldwide interest as a promising method for conversion of solar energy into chemical fuels.^{1–4} In order to utilize solar energy effectively, a photocatalyst must harvest visible light of up to 600 nm or even longer.² Z-scheme water splitting systems based on two-step photoexcitation are typically composed of a H_2 evolution photocatalyst, an O_2 evolution photocatalyst, and electron mediators.^{3,4} During photoexcitation, electrons reduce H^+ to H_2 and holes oxidize the reduced form of redox mediators on the H_2 evolution photocatalyst, while on the O_2 evolution photocatalyst, electrons reduce the oxidized form of redox mediators and holes oxidize H_2O to O_2 . It has also been found that Z-scheme water splitting can complete even in the absence of redox couples owing to the interparticle electron transfer,

where holes in a H_2 evolution photocatalyst and electrons in an O_2 evolution photocatalyst recombine *via* physical contact.^{4,5} Compared to the one-step excitation mechanism that uses a single visible-light-responsive photocatalyst, the two-step excitation mechanism has several advantages:⁶ it enables the use of a semiconductor that is active for either water reduction or oxidation alone as long as it is active for the oxidation or reduction of the redox mediators, respectively. Because the energy required to drive either photocatalyst can be lower, a wider range of visible-light-active photocatalysts are applicable. For example, WO_3 , BiVO_4 , and Rh-doped SrTiO_3 have been employed in Z-scheme water splitting although they are active only for H_2 or O_2 evolution in the presence of appropriate sacrificial reagents.^{6–8} Photocatalysts that are capable of both the H_2 and O_2 evolution reactions with sacrificial reagents are also applicable to Z-scheme water splitting, as has been demonstrated with TaON ^{6,9} and Ta_3N_5 .¹⁰ Moreover, H_2 and O_2 are generated on different photocatalysts, which could in principle offer a simple means of separating the gaseous products using an appropriate membrane filter.⁸ Much effort has been devoted to construction of efficient Z-scheme systems by developing new materials and efficient electron relays.

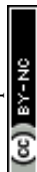
$\text{Sm}_2\text{Ti}_2\text{S}_2\text{O}_5$, an oxysulphide semiconductor photocatalyst, has a crystal structure similar to that of a Ruddlesden–Popper-type layered perovskite oxide.¹¹ Under visible light irradiation ($\lambda < 650$ nm), $\text{Sm}_2\text{Ti}_2\text{S}_2\text{O}_5$ can evolve H_2 or O_2 from aqueous solutions containing sacrificial electron donors (Na_2S – Na_2SO_3 or methanol) or acceptors (Ag^+), respectively.¹¹ This indicates

^a Department of Chemical System Engineering, The University of Tokyo, 7-3-1 Hongo, Bunkyo-ku, Tokyo 113-8656, Japan. E-mail: domen@chemsys.t.u-tokyo.ac.jp

^b Precursory Research for Embryonic Science and Technology (PRESTO), Japan Science and Technology Agency (JST), 4-1-8 Honcho Kawaguchi, Saitama 332-0012, Japan

[†] Current address: Department of Chemistry, Graduate School of Science and Engineering, Tokyo Institute of Technology, 2-12-1-NE-2 Ookayama, Meguro-ku, Tokyo 152-8550, Japan.

[‡] Current address: State Key Laboratory of Catalysis, Dalian National Laboratory for Clean Energy, Dalian Institute of Chemical Physics, Chinese Academy of Sciences, Zhongshan Road 457, Dalian 116023, China.



that $\text{Sm}_2\text{Ti}_2\text{S}_2\text{O}_5$ has band positions suitable for water splitting under visible light irradiation. However, $\text{Sm}_2\text{Ti}_2\text{S}_2\text{O}_5$ and other oxysulphides have not been applied to Z-scheme water splitting successfully. Earlier studies on the photocatalyst $\text{Sm}_2\text{Ti}_2\text{S}_2\text{O}_5$ involved the H_2S gas sulphurization method for the preparation of fine $\text{Sm}_2\text{Ti}_2\text{S}_2\text{O}_5$ particles,¹² and the loading and addition of various metal species to $\text{Sm}_2\text{Ti}_2\text{S}_2\text{O}_5$.^{13–15} It was found that promoting both the photocatalytic reduction of water and the oxidation of sacrificial electron donors as well as reducing the defect density of $\text{Sm}_2\text{Ti}_2\text{S}_2\text{O}_5$ were important for improving the photocatalytic H_2 evolution rate on $\text{Sm}_2\text{Ti}_2\text{S}_2\text{O}_5$ from an aqueous solution of Na_2S and Na_2SO_3 . In this study, methods of modifying $\text{Sm}_2\text{Ti}_2\text{S}_2\text{O}_5$ were investigated to improve the H_2 evolution activity. After appropriate post-treatments such as annealing with sulphur and etching with nitric acid, $\text{Sm}_2\text{Ti}_2\text{S}_2\text{O}_5$ loaded with Rh exhibited a higher activity for the sacrificial H_2 evolution reaction. The modified $\text{Sm}_2\text{Ti}_2\text{S}_2\text{O}_5$ was used as a H_2 evolution photocatalyst in Z-scheme water splitting. It was found that Pt-loaded $\text{Sm}_2\text{Ti}_2\text{S}_2\text{O}_5$ suspended with TiO_2 (rutile) in an aqueous NaI solution was capable of splitting water into H_2 and O_2 under UV irradiation ($\lambda > 300$ nm).

Experimental

Amorphous $\text{Sm}_2\text{Ti}_2\text{O}_7$ was synthesized as an oxide precursor by a polymerized complex method.¹² Titanium tetraisopropoxide (0.02 mol, Kanto Chemical Co., 97%) and anhydrous citric acid (0.3 mol, Wako Pure Chemicals, 98%) were dissolved in ethylene glycol (0.2 mol, Kanto Chemical Co., 99.5%) at room temperature, and the mixture was heated at 333 K until the reagents were completely dissolved. Subsequently, $\text{Sm}(\text{NO}_3)_3 \cdot 6\text{H}_2\text{O}$ (0.02 mol, Wako Pure Chemicals Co., 99.5%) and 20 mL methanol were added to the solution. The mixture was stirred at 403 K until a transparent gel was formed. It was polymerized and carbonized at 523, 573, and 623 K for 1 h each and finally calcined at 773 K for 12 h to remove the carbon completely. The resulting amorphous oxide was sulphurized at 1223 K for 1 h under a flow of H_2S (10 mL min^{-1}) and calcined for 2 h in air at 573 K.

As-synthesized $\text{Sm}_2\text{Ti}_2\text{S}_2\text{O}_5$ was sealed in evacuated quartz tubes with 5 wt% sulphur powder (High Purity Chemicals Co., 99.99%) with respect to $\text{Sm}_2\text{Ti}_2\text{S}_2\text{O}_5$ and annealed at 1223 K for 20 h.¹² Nitric acid treatment was conducted by dispersing $\text{Sm}_2\text{Ti}_2\text{S}_2\text{O}_5$ powder (ca. 0.5 g) in HNO_3 (Wako Pure Chemicals Co., 69.8 wt%) for 10 min at room temperature, followed by rinsing with distilled water, filtration, drying at 343 K, and heat treatment at 573 K for 1 h in air. The mass loss during the whole nitric acid etching procedure was approximately 40%, while the mass loss during the rinsing and filtration procedures was approximately 8%. When both treatments were carried out, the nitric acid etching was performed after the sulphur annealing. $\text{Sm}_2\text{Ti}_2\text{S}_2\text{O}_5$ samples subjected to the sulphur annealing alone, to the nitric acid etching alone, and to both procedures will hereafter be denoted as $\text{Sm}_2\text{Ti}_2\text{S}_2\text{O}_5$ (S), $\text{Sm}_2\text{Ti}_2\text{S}_2\text{O}_5$ (HNO_3), and $\text{Sm}_2\text{Ti}_2\text{S}_2\text{O}_5$ (S + HNO_3), respectively.

The samples were characterized using X-ray powder diffraction (XRD; RINT-Ultima III, Rigaku; $\text{Cu K}\alpha$), ultraviolet-visible

diffuse-reflectance spectroscopy (DRS; V-670, JASCO), field-emission scanning electron microscopy (FE-SEM; S-4700, Hitachi) and X-ray photoelectron spectroscopy (XPS; JPS-9000, JEOL). The binding energy for each sample was corrected by the reference C 1s peak (285.0 eV). The peak areas of Sm 3d_{5/2}, Ti 2p, S 2p_{3/2}, and O 1s were acquired by integrating the signals over 1090.0–1077.0, 468.0–455.8, 171.8–157.4, and 535.7–526.5 eV, respectively.

The photocatalytic H_2 evolution reactions were carried out in an inner irradiation-type Pyrex reaction vessel connected to an air-tight closed gas circulation system made of Pyrex glass. An aqueous solution (400 mL) containing the photocatalyst sample (0.2 g), Na_2S – Na_2SO_3 (0.2 M each) was irradiated with a 450 W high-pressure Hg lamp through a NaNO_2 solution (2 M) as an optical filter, the cutoff wavelength of which was 400 nm. For the H_2 evolution reaction, Rh (1.5 wt%) was loaded as a H_2 evolution cocatalyst by photodeposition from the Na_2S – Na_2SO_3 aqueous solutions.^{13,14} A calculated amount of $\text{RhCl}_3 \cdot x\text{H}_2\text{O}$ (Aldrich, 38–40% as Rh) precursor added to the solution was reduced to metallic Rh by photoexcited electrons from the photocatalyst in the initial stage of the reaction. The reactant solution was maintained at room temperature by flowing cooling water during the reaction. The evolved gas was analyzed by gas chromatography (GC, TCD, Shimadzu).

For Z-scheme water splitting, Pt-loaded $\text{Sm}_2\text{Ti}_2\text{S}_2\text{O}_5$ (0.2 g), rutile TiO_2 (0.2 g), and NaI (50 mM) were used as a H_2 evolution photocatalyst, O_2 evolution photocatalyst, and redox mediator, respectively. Pt is employed as an effective H_2 evolution cocatalyst in Z-scheme water splitting involving the redox couple IO_3^-/I^- .^{6,10,15–17} Pt (2 wt%) was photodeposited on $\text{Sm}_2\text{Ti}_2\text{S}_2\text{O}_5$ from a calculated amount of $\text{H}_2\text{PtCl}_6 \cdot 6\text{H}_2\text{O}$ (Aldrich, 38–40% Pt) in an aqueous NaI solution (pH = 6). The platinized sample was collected and used for Z-scheme water splitting. The pH of the solution containing the H_2 evolution photocatalyst, O_2 evolution photocatalyst, and redox mediator was adjusted using an aqueous NaOH solution. The solution was evacuated and irradiated with a 450 W high-pressure Hg lamp ($\lambda > 300$ nm). Note that conventional TiO_2 (rutile) was employed to assess the applicability of $\text{Sm}_2\text{Ti}_2\text{S}_2\text{O}_5$ as a H_2 evolution photocatalyst in Z-scheme water splitting, since rutile-type TiO_2 worked effectively as an O_2 evolution photocatalyst in Z-scheme systems involving IO_3^-/I^- owing to preferential adsorption of IO_3^- ions onto rutile-type TiO_2 and its sufficient activity of for IO_3^- reduction even without elaborate modifications while necessitating UV illumination.¹⁷

Results and discussion

Effects of post-treatments

Fig. 1 shows XRD patterns of the $\text{Sm}_2\text{Ti}_2\text{S}_2\text{O}_5$ samples before and after the post-treatments. The diffraction profile of the $\text{Sm}_2\text{Ti}_2\text{S}_2\text{O}_5$ phase was unchanged and no impurity phase was generated by the post-treatments. The peak intensities of $\text{Sm}_2\text{Ti}_2\text{S}_2\text{O}_5$ and $\text{Sm}_2\text{Ti}_2\text{S}_2\text{O}_5$ (HNO_3) were identical, while those of $\text{Sm}_2\text{Ti}_2\text{S}_2\text{O}_5$ (S) and $\text{Sm}_2\text{Ti}_2\text{S}_2\text{O}_5$ (S + HNO_3) became somewhat stronger. This suggests that the sulphur annealing at 1223 K improved the crystallinity of $\text{Sm}_2\text{Ti}_2\text{S}_2\text{O}_5$ and that the



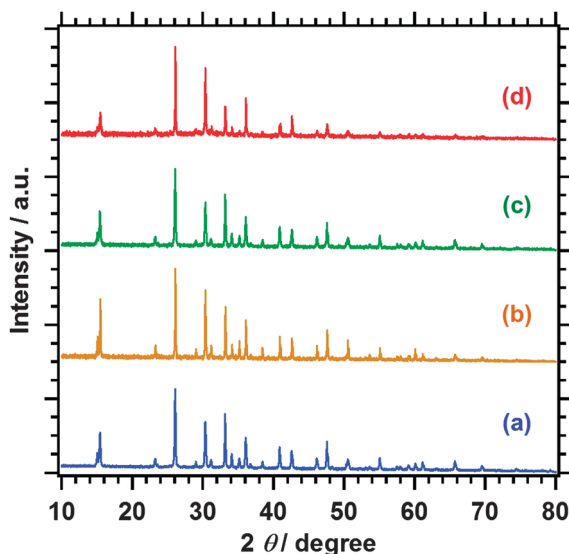


Fig. 1 XRD patterns of (a) $\text{Sm}_2\text{Ti}_2\text{S}_2\text{O}_5$, (b) $\text{Sm}_2\text{Ti}_2\text{S}_2\text{O}_5$ (S), (c) $\text{Sm}_2\text{Ti}_2\text{S}_2\text{O}_5$ (HNO_3), and (d) $\text{Sm}_2\text{Ti}_2\text{S}_2\text{O}_5$ (S + HNO_3).

nitric acid etching did not change the bulk crystallinity of $\text{Sm}_2\text{Ti}_2\text{S}_2\text{O}_5$.

Fig. 2 shows SEM images of the corresponding $\text{Sm}_2\text{Ti}_2\text{S}_2\text{O}_5$ samples. $\text{Sm}_2\text{Ti}_2\text{S}_2\text{O}_5$ consisted of plate-like submicron particles, which formed massive secondary particles several micrometers in size. During the sulphur annealing, these aggregates were sintered into 0.5–1 μm particles with smoother surfaces. When the samples were etched with HNO_3 , dramatic changes were observed in the surface morphologies of $\text{Sm}_2\text{Ti}_2\text{S}_2\text{O}_5$ and $\text{Sm}_2\text{Ti}_2\text{S}_2\text{O}_5$ (S). It appeared that the outer surface of the samples had dissolved, exposing the interior consisting of submicron $\text{Sm}_2\text{Ti}_2\text{S}_2\text{O}_5$ grains. This verified the speculation of our previous study that the large $\text{Sm}_2\text{Ti}_2\text{S}_2\text{O}_5$ (S) particles were polycrystalline.¹² The $\text{Sm}_2\text{Ti}_2\text{S}_2\text{O}_5$ (S + HNO_3) grains were, on average, larger than the $\text{Sm}_2\text{Ti}_2\text{S}_2\text{O}_5$ (HNO_3) grains.

The surface compositions of the $\text{Sm}_2\text{Ti}_2\text{S}_2\text{O}_5$ samples before and after the post-treatments are tabulated in Table 1. Pristine

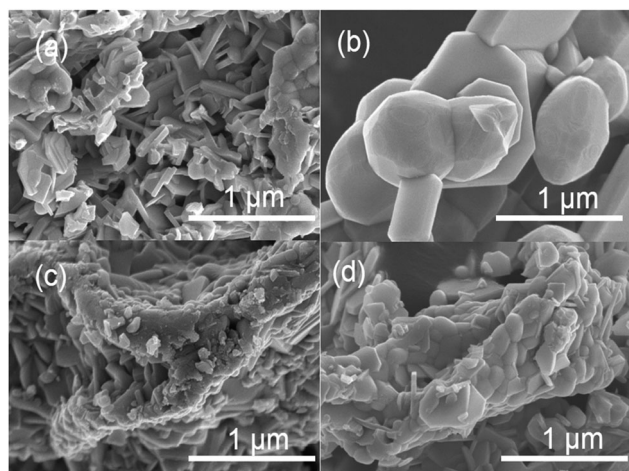


Fig. 2 SEM images of (a) $\text{Sm}_2\text{Ti}_2\text{S}_2\text{O}_5$, (b) $\text{Sm}_2\text{Ti}_2\text{S}_2\text{O}_5$ (S), (c) $\text{Sm}_2\text{Ti}_2\text{S}_2\text{O}_5$ (HNO_3), and (d) $\text{Sm}_2\text{Ti}_2\text{S}_2\text{O}_5$ (S + HNO_3).

Table 1 Surface atomic ratios of $\text{Sm}_2\text{Ti}_2\text{S}_2\text{O}_5$ before and after the post-treatments, as estimated by XPS

Sample	Sm/Ti	S/Ti	O/Ti
$\text{Sm}_2\text{Ti}_2\text{S}_2\text{O}_5$	1.1	1.9	6.6
$\text{Sm}_2\text{Ti}_2\text{S}_2\text{O}_5$ (HNO_3)	0.6	2.2	5.8
$\text{Sm}_2\text{Ti}_2\text{S}_2\text{O}_5$ (S)	0.9	2.6	7.5
$\text{Sm}_2\text{Ti}_2\text{S}_2\text{O}_5$ (S + HNO_3)	0.9	2.0	6.5

$\text{Sm}_2\text{Ti}_2\text{S}_2\text{O}_5$ nearly exhibited the stoichiometric Sm/Ti ratio, while the S/Ti and O/Ti ratios were larger than the corresponding stoichiometric ratios. We obtained similar results in our previous study.¹² This is because the $\text{Sm}_2\text{Ti}_2\text{S}_2\text{O}_5$ surface was enriched with elemental and oxidized sulphur species when $\text{Sm}_2\text{Ti}_2\text{S}_2\text{O}_5$ was sulphurized under a H_2S flow and annealed in air. $\text{Sm}_2\text{Ti}_2\text{S}_2\text{O}_5$ (HNO_3) after the nitric acid etching exhibited a smaller Sm/Ti ratio than pristine $\text{Sm}_2\text{Ti}_2\text{S}_2\text{O}_5$. This indicates that the $\text{Sm}_2\text{Ti}_2\text{S}_2\text{O}_5$ surface was indeed dissolved by nitric acid, particularly the Sm component with weak basicity. The sulphur annealing did not change the surface Sm/Ti ratio significantly, while generating excessive sulphur on the surface of $\text{Sm}_2\text{Ti}_2\text{S}_2\text{O}_5$ (S). $\text{Sm}_2\text{Ti}_2\text{S}_2\text{O}_5$ (S + HNO_3) maintained the Sm/Ti ratio of $\text{Sm}_2\text{Ti}_2\text{S}_2\text{O}_5$ (S), unlike the case of $\text{Sm}_2\text{Ti}_2\text{S}_2\text{O}_5$ (HNO_3) after the nitric acid treatment. It is thought that a part of the pristine $\text{Sm}_2\text{Ti}_2\text{S}_2\text{O}_5$ sample was rather amorphous and thus the nitric acid etching resulted in preferential dissolution of Sm species. However, annealing in the presence of sulphur improved the crystallinity of $\text{Sm}_2\text{Ti}_2\text{S}_2\text{O}_5$, incorporating amorphous Sm species into the crystal structure, thereby suppressing the leaching of Sm species during the nitric acid treatment. Note that the surface of $\text{Sm}_2\text{Ti}_2\text{S}_2\text{O}_5$ (S) was still etched, as was evident from the SEM images. This resulted in the partial removal of the excess sulphur species on the surface.

The DRS shown in Fig. 3 confirms that the pristine sample exhibited a light absorption onset at approximately 650 nm, which corresponded to the band gap transition of $\text{Sm}_2\text{Ti}_2\text{S}_2\text{O}_5$.¹¹ The background absorption was also observed, presumably because of reduced Ti species. The reduced Ti species may have been generated by the exposure to heated H_2S .¹² $\text{Sm}_2\text{Ti}_2\text{S}_2\text{O}_5$ (HNO_3) had a similar absorption onset and background absorption. The fact that etching of the surface did not weaken the background absorption indicates that the reduced Ti species were present in the bulk of the sample. $\text{Sm}_2\text{Ti}_2\text{S}_2\text{O}_5$ (S) and $\text{Sm}_2\text{Ti}_2\text{S}_2\text{O}_5$ (S + HNO_3), which were subjected to the sulphur annealing treatment, had similar absorption onsets but lower background absorption. Considering the dramatic changes in morphology that occurred during the sulphur annealing, it is reasonable to assume that the reduced Ti species in the bulk were oxidized by elemental sulphur upon annealing at 1223 K.

Fig. 4 shows the reaction time courses of photocatalytic H_2 evolution using pristine and post-treated $\text{Sm}_2\text{Ti}_2\text{S}_2\text{O}_5$ samples. The photocatalytic activity of $\text{Sm}_2\text{Ti}_2\text{S}_2\text{O}_5$ was improved by the sulphur annealing and the nitric acid etching, and combining these post-treatments resulted in the highest activity. During the sulphurization of amorphous $\text{Sm}_2\text{Ti}_2\text{O}_7$ to $\text{Sm}_2\text{Ti}_2\text{S}_2\text{O}_5$, a certain amount of Ti^{3+} species was generated because of the



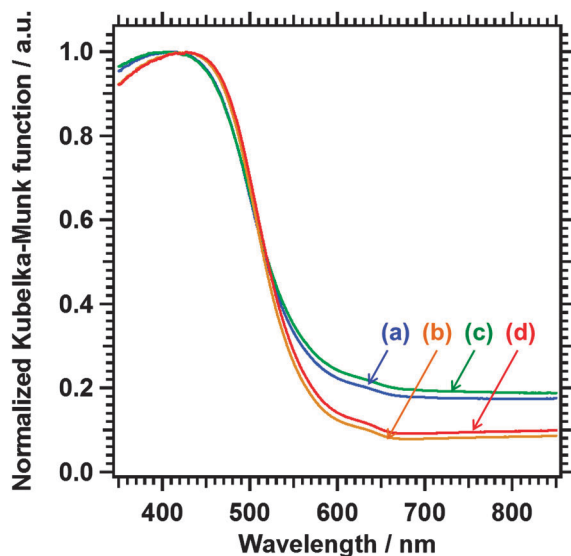


Fig. 3 UV-vis DRS of (a) $\text{Sm}_2\text{Ti}_2\text{S}_2\text{O}_5$, (b) $\text{Sm}_2\text{Ti}_2\text{S}_2\text{O}_5$ (S), (c) $\text{Sm}_2\text{Ti}_2\text{S}_2\text{O}_5$ (HNO_3), and (d) $\text{Sm}_2\text{Ti}_2\text{S}_2\text{O}_5$ (S + HNO_3).

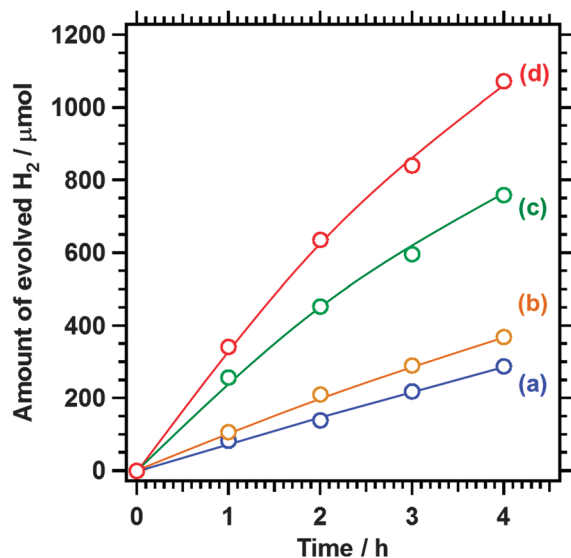


Fig. 4 Time courses of H_2 evolution over $\text{Sm}_2\text{Ti}_2\text{S}_2\text{O}_5$ after various post-treatments: (a) $\text{Sm}_2\text{Ti}_2\text{S}_2\text{O}_5$, (b) $\text{Sm}_2\text{Ti}_2\text{S}_2\text{O}_5$ (S), (c) $\text{Sm}_2\text{Ti}_2\text{S}_2\text{O}_5$ (HNO_3), and (d) $\text{Sm}_2\text{Ti}_2\text{S}_2\text{O}_5$ (S + HNO_3). Reaction conditions: catalyst, 0.2 g; cocatalyst, 1.5 wt% Rh (*in situ* photodeposition); sacrificial electron donor, Na_2S + Na_2SO_3 (0.2 M each in 400 mL of water); light source, 450 W high-pressure Hg lamp ($\lambda > 400$ nm, 2 M NaNO_2 (aq.) as a filter solution).

reduction of Ti^{4+} under the heated H_2S atmosphere. The generation of reduced Ti species is accompanied by the formation of anion vacancies. These vacancies tend to act as recombination centres for photoexcited electrons and holes and suppress the photocatalytic activity.^{12,13} The sulphur annealing can potentially produce a higher activity owing to the lower density of reduced Ti species in $\text{Sm}_2\text{Ti}_2\text{S}_2\text{O}_5$. In reality, however, hardly any activity enhancement was observed upon sulphur annealing. This is likely due to the presence of excess sulphur species on the surface, which blocked the surface active sites and thus prevented the deposition

of Rh as H_2 evolution sites.¹² The sintering of $\text{Sm}_2\text{Ti}_2\text{S}_2\text{O}_5$ may also have led to the lower-than-expected photocatalytic activity.¹² The nitric acid etching improved the H_2 evolution activity by a factor of three although the Sm component was deficient on the sample surface. The SEM and XPS results suggest that the enhanced activity of $\text{Sm}_2\text{Ti}_2\text{S}_2\text{O}_5$ (HNO_3) is attributable to the elimination of the defective amorphous layers on the surface that would otherwise have prevented charge transfer. $\text{Sm}_2\text{Ti}_2\text{S}_2\text{O}_5$ (S + HNO_3) benefited from both post-treatments. Moreover, the excess sulphur species on $\text{Sm}_2\text{Ti}_2\text{S}_2\text{O}_5$ (S) were eliminated in part by the nitric acid etching, and the Sm deficiency on the surface observed in the case of $\text{Sm}_2\text{Ti}_2\text{S}_2\text{O}_5$ (HNO_3) was avoided owing to the improved crystallinity. As a result, $\text{Sm}_2\text{Ti}_2\text{S}_2\text{O}_5$ (S + HNO_3) showed a H_2 evolution rate that was 4.5 times higher than that of pristine $\text{Sm}_2\text{Ti}_2\text{S}_2\text{O}_5$.

Application of $\text{Sm}_2\text{Ti}_2\text{S}_2\text{O}_5$ to Z-scheme water splitting

Table 2 shows the amounts of H_2 and O_2 evolved in Z-scheme water splitting reactions over 5 h using Pt-loaded $\text{Sm}_2\text{Ti}_2\text{S}_2\text{O}_5$ samples as a H_2 evolution photocatalyst. Simultaneous evolution of H_2 and O_2 was observed only when $\text{Sm}_2\text{Ti}_2\text{S}_2\text{O}_5$ (S + HNO_3) was used as a H_2 evolution photocatalyst together with TiO_2 (rutile) as an O_2 evolution photocatalyst and NaI as a redox mediator. The ratio of H_2 to O_2 produced was higher than the stoichiometry of overall water splitting because of the presence of excess electron donors (NaI) in the beginning of the reaction. When one of the components, *i.e.*, the H_2 evolution photocatalyst, O_2 evolution photocatalyst, or redox mediator, was missing, the gas evolution was negligible. This confirms that the water splitting reaction occurred *via* the Z-scheme mechanism.

The use of pristine $\text{Sm}_2\text{Ti}_2\text{S}_2\text{O}_5$, $\text{Sm}_2\text{Ti}_2\text{S}_2\text{O}_5$ (S), and $\text{Sm}_2\text{Ti}_2\text{S}_2\text{O}_5$ (HNO_3) did not lead to successful O_2 evolution, while producing a certain amount of H_2 . In addition, the H_2 evolution ceased during the initial stage of the reaction. In Z-scheme water splitting in the presence of reversible redox couples, simultaneous evolution of H_2 and O_2 is often difficult because of backward reactions on the respective photocatalysts. IO_3^- produced by the oxidation of I^- on $\text{Sm}_2\text{Ti}_2\text{S}_2\text{O}_5$ could largely be reduced back to I^- unless the H_2 evolution activity was high enough to outweigh the thermodynamically favorable

Table 2 Photocatalytic activity for Z-scheme water splitting using $\text{Sm}_2\text{Ti}_2\text{S}_2\text{O}_5$ ^a

H_2 evolution photocatalyst ^b	O_2 evolution photocatalyst	Redox mediator	Activity ^c /μmol	
			H_2	O_2
$\text{Sm}_2\text{Ti}_2\text{S}_2\text{O}_5$	TiO_2 (rutile)	NaI	10	0
$\text{Sm}_2\text{Ti}_2\text{S}_2\text{O}_5$ (S)	TiO_2 (rutile)	NaI	13	0
$\text{Sm}_2\text{Ti}_2\text{S}_2\text{O}_5$ (HNO_3)	TiO_2 (rutile)	NaI	11	0
$\text{Sm}_2\text{Ti}_2\text{S}_2\text{O}_5$ (S + HNO_3)	TiO_2 (rutile)	NaI	45	16
None	TiO_2 (rutile)	NaI	0	0
$\text{Sm}_2\text{Ti}_2\text{S}_2\text{O}_5$ (S + HNO_3)	None	NaI	0.6	0
$\text{Sm}_2\text{Ti}_2\text{S}_2\text{O}_5$ (S + HNO_3)	TiO_2 (rutile)	None	0	0

^a Reaction conditions: photocatalysts, 0.2 g each; reaction solution, aqueous NaI solution (430 mL, 50 mM, pH = 12); light source, 450 W high-pressure Hg lamp. ^b Loaded with 2 wt% of Pt by photodeposition. ^c Estimated from the amount of gases evolved in 5 h.



backward reaction. In addition, the oxygen evolution on rutile-type TiO_2 could be suppressed by the oxidation of I^- when the concentration of I^- was high.¹⁷ The absence of O_2 evolution thus suggests that the activities of the above three $\text{Sm}_2\text{Ti}_2\text{S}_2\text{O}_5$ samples for H_2 evolution and I^- oxidation were too low to provide a sufficient amount of IO_3^- in the reaction solution. Further characterization is necessary to determine why, among the $\text{Sm}_2\text{Ti}_2\text{S}_2\text{O}_5$ samples subjected to different post-treatments, only $\text{Sm}_2\text{Ti}_2\text{S}_2\text{O}_5$ ($\text{S} + \text{HNO}_3$) was active for Z-scheme water splitting. However, the present results suffice to show that the appropriate post-treatments enabled the oxysulphide photocatalyst to be used as a H_2 evolution photocatalyst for Z-scheme water splitting and that lowering the densities of both reduced Ti species and surface impurities was necessary.

Fig. 5 shows the dependence of the photocatalytic activity of the Z-scheme system for water splitting on the pH of the reaction solution. Z-scheme water splitting was enhanced significantly as the pH increased from 6 to 12 and was suppressed at $\text{pH} > 12$. O_2 evolution was almost negligible at $\text{pH} < 9$. This is because the main oxidative product on Pt-loaded $\text{Sm}_2\text{Ti}_2\text{S}_2\text{O}_5$ ($\text{S} + \text{HNO}_3$) was I_3^- , which failed to serve as an efficient electron acceptor for O_2 evolution over rutile TiO_2 . The photocatalytic activity decreased at $\text{pH} > 12$. This is probably because of the decreasing driving force of $\text{Sm}_2\text{Ti}_2\text{S}_2\text{O}_5$ for H_2 evolution with increasing pH. It has been found previously that the potential of the band gap of $\text{Sm}_2\text{Ti}_2\text{S}_2\text{O}_5$ was independent of the pH of the solution,¹¹ while the H_2 evolution potential shifted negatively with increasing pH. Thus, a basic solution at a pH of around 11–12 was the most favourable for Z-scheme water splitting using $\text{Sm}_2\text{Ti}_2\text{S}_2\text{O}_5$, TiO_2 , and I^-/IO_3^- .

Fig. 6 shows the results of Z-scheme water splitting with intermittent evacuations. The ratio of H_2 and O_2 approached

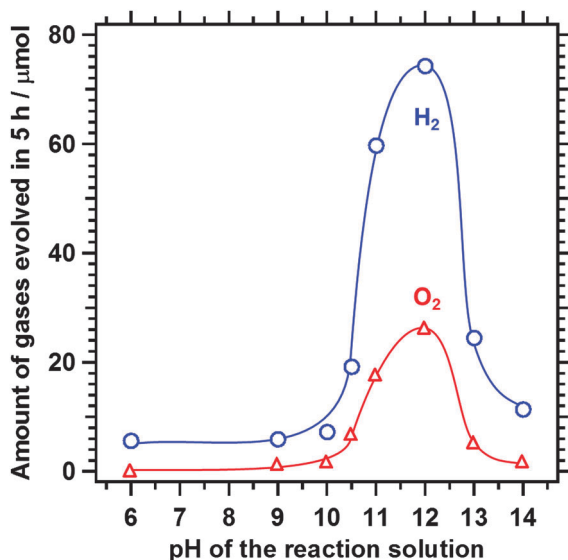


Fig. 5 pH dependence of photocatalytic activity of the Z-scheme system based on 2 wt% Pt-loaded $\text{Sm}_2\text{Ti}_2\text{S}_2\text{O}_5$ ($\text{S} + \text{HNO}_3$), TiO_2 (rutile), and NaI under UV light illumination. Reaction conditions: photocatalysts, 0.2 g each; solution, aqueous NaI solution (50 mM, 430 mL); light source: 450 W high-pressure Hg lamp ($\lambda > 300$ nm).

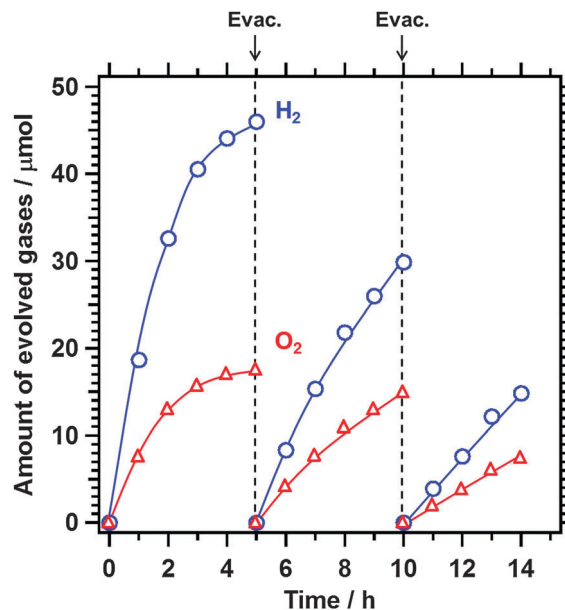


Fig. 6 Time course of Z-scheme water splitting using 2 wt% Pt-loaded $\text{Sm}_2\text{Ti}_2\text{S}_2\text{O}_5$ ($\text{S} + \text{HNO}_3$), TiO_2 (rutile), and NaI under UV light illumination. Reaction conditions: photocatalysts, 0.2 g each; reaction solution, aqueous NaI solution (50 mM, pH = 11, 430 mL); light source: 450 W high-pressure Hg lamp ($\lambda > 300$ nm).

2 : 1 after the first five-hour reaction and subsequent evacuation as the excess I^- was converted into IO_3^- during the reaction. The rate of gas evolution gradually decreased as the gas product accumulated in the closed system because the backward reaction from H_2 and O_2 to H_2O occurred on the Pt used as a cocatalyst. The rate of water splitting recovered to some extent upon evacuation. However, the photocatalytic activity of the system gradually decreased. XRD patterns presented in Fig. 7 show that the sample after the reaction was a mixture of $\text{Sm}_2\text{Ti}_2\text{S}_2\text{O}_5$

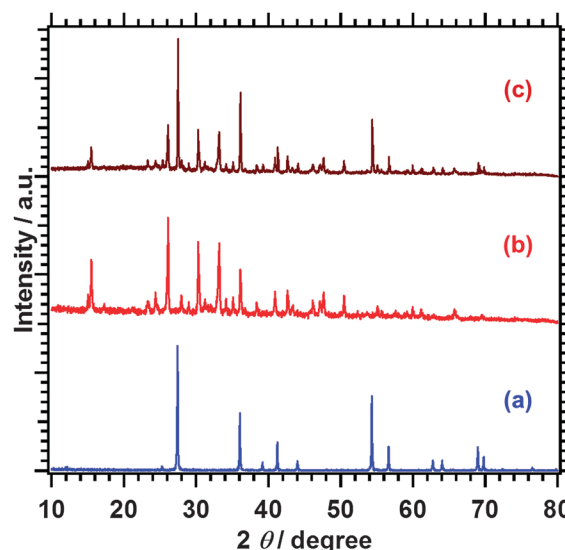


Fig. 7 XRD patterns of (a) rutile-type TiO_2 , (b) $\text{Sm}_2\text{Ti}_2\text{S}_2\text{O}_5$ ($\text{S} + \text{HNO}_3$), and (c) after the Z-scheme water splitting reaction with rutile-type TiO_2 at pH 11.



(S + HNO₃) and rutile-type TiO₂. This result suggests that the bulk of Sm₂Ti₂S₂O₅ (S + HNO₃) was mostly stable during the water splitting reaction. The deactivation may be due to the photo-oxidation of the surface of Sm₂Ti₂S₂O₅ by photoexcited holes under the intense UV illumination. Although UV illumination and stabilization of Sm₂Ti₂S₂O₅ were still necessary, this represents the first instance of Z-scheme water splitting achieved using an oxysulphide photocatalyst as a H₂ evolution photocatalyst. It is expected that dual cocatalyst loading on Sm₂Ti₂S₂O₅^{18,19} and the use of visible-light-sensitive O₂ evolution photocatalysts will allow stable water splitting under visible light illumination.

Conclusions

The processes of annealing with sulphur and etching with nitric acid were studied to improve the photocatalytic activity of Sm₂Ti₂S₂O₅ for H₂ evolution in sacrificial water reduction and Z-scheme water splitting. The photocatalytic activity improved by a factor of 4.5 when the sulphur annealing and nitric acid etching were applied in combination. The effects of these post-treatments were attributed to the oxidation of reduced Ti³⁺ species and the removal of amorphous surface phases and excess sulphur species, respectively.

Following the sulphur annealing and the nitric acid etching, Sm₂Ti₂S₂O₅ could be used as a H₂ evolution photocatalyst in Z-scheme water splitting in combination with TiO₂ as an O₂ evolution photocatalyst and NaI as a redox mediator. All three of the components were necessary to drive Z-scheme water splitting. Employing both post-treatments was essential for successful Z-scheme water splitting, which indicated the importance of removing reduced Ti³⁺ species and surface impurities from Sm₂Ti₂S₂O₅. Although UV irradiation was necessary because of the use of TiO₂, the present study revealed that appropriate modifications allowed an oxysulphide photocatalyst to serve as a H₂ evolution photocatalyst in Z-scheme water splitting.

Acknowledgements

This work was financially supported by the Grant-in-Aid for Specially Promoted Research (no. 23000009) of the Japan Society for the Promotion of Science (JSPS) and the Advanced Low Carbon Technology Research and Development Program (ALCA) of the Japan Science and Technology Agency (JST). Further financial support was provided by JSPS through the Funding Program for World-Leading Innovative R&D on

Science and Technology (FIRST), initiated by the Council for Science and Technology Policy (CSTP), and by an international exchange program of the A3 Foresight Program of JSPS. Z.W. gratefully acknowledges Dr Curulla-Ferre, Prof. Wimmer, and Dr Yagi of TOTAL S.A. for scientific discussions and financial support. K. M. is indebted to the Nippon Sheet Glass Foundation for Materials Science and Engineering for funding support.

Notes and references

- 1 A. Kudo and Y. Miseki, *Chem. Soc. Rev.*, 2009, **38**, 253.
- 2 K. Maeda and K. Domen, *J. Phys. Chem. Lett.*, 2010, 2655.
- 3 R. Abe, *J. Photochem. Photobiol., C*, 2010, **11**, 179.
- 4 K. Maeda, *ACS Catal.*, 2013, **3**, 1486.
- 5 Y. Sasaki, H. Nemoto, K. Saito and A. Kudo, *J. Phys. Chem. C*, 2009, **113**, 17536.
- 6 K. Maeda, M. Higashi, D. Lu, R. Abe and K. Domen, *J. Am. Chem. Soc.*, 2010, **132**, 5858.
- 7 Y. Sasaki, A. Iwase, H. Kato and A. Kudo, *J. Catal.*, 2008, **259**, 133.
- 8 Y. Sasaki, H. Kato and A. Kudo, *J. Am. Chem. Soc.*, 2013, **135**, 5441.
- 9 M. Higashi, R. Abe, A. Ishikawa, T. Takata, B. Ohtani and K. Domen, *Chem. Lett.*, 2008, **37**, 138.
- 10 M. Tabata, K. Maeda, M. Higashi, D. Lu, T. Takata, R. Abe and K. Domen, *Langmuir*, 2010, **26**, 9161.
- 11 A. Ishikawa, T. Takata, J. N. Kondo, M. Hara, H. Kobayashi and K. Domen, *J. Am. Chem. Soc.*, 2002, **124**, 13547.
- 12 A. Ishikawa, Y. Yamada, T. Takata, J. N. Kondo, M. Hara, H. Kobayashi and K. Domen, *Chem. Mater.*, 2003, **15**, 4442.
- 13 F. Zhang, K. Maeda, T. Takata and K. Domen, *J. Catal.*, 2011, **280**, 1.
- 14 F. Zhang, K. Maeda, T. Takata, T. Hisatomi and K. Domen, *Catal. Today*, 2012, **185**, 253.
- 15 K. Sayama, K. Mukasa, R. Abe, Y. Abe and H. Arakawa, *Chem. Commun.*, 2001, 2416.
- 16 K. Sayama, K. Mukasa, R. Abe, Y. Abe and H. Arakawa, *J. Photochem. Photobiol., A*, 2002, **148**, 71.
- 17 R. Abe, K. Sayama and H. Sugihara, *J. Phys. Chem. B*, 2005, **109**, 16052.
- 18 F. Zhang, K. Maeda, T. Takata and K. Domen, *Chem. Commun.*, 2010, **46**, 7313.
- 19 R. Li, Z. Chen, W. Zhao, F. Zhang, K. Maeda, B. Huang, S. Shen, K. Domen and C. Li, *J. Phys. Chem. C*, 2013, **117**, 376.

